



Apparent diffusion coefficient value for a B-cell central nervous system lymphoma in a cat

Authors: Tanaka, Toshiyuki, Akiyoshi, Hideo, Shimazaki, Hitoshi, Kawakami, Ryo, Mie, Keiichiro, et al.

Source: Journal of Feline Medicine and Surgery Open Reports, 4(1)

Published By: SAGE Publishing

URL: <https://doi.org/10.1177/2055116917750762>

BioOne Complete (complete.BioOne.org) is a full-text database of 200 subscribed and open-access titles in the biological, ecological, and environmental sciences published by nonprofit societies, associations, museums, institutions, and presses.

Your use of this PDF, the BioOne Complete website, and all posted and associated content indicates your acceptance of BioOne's Terms of Use, available at www.bioone.org/terms-of-use.

Usage of BioOne Complete content is strictly limited to personal, educational, and non - commercial use. Commercial inquiries or rights and permissions requests should be directed to the individual publisher as copyright holder.

BioOne sees sustainable scholarly publishing as an inherently collaborative enterprise connecting authors, nonprofit publishers, academic institutions, research libraries, and research funders in the common goal of maximizing access to critical research.



Apparent diffusion coefficient value for a B-cell central nervous system lymphoma in a cat

Journal of Feline Medicine and Surgery Open Reports
1–5

© The Author(s) 2018

Reprints and permissions:

sagepub.co.uk/journalsPermissions.nav

DOI: 10.1177/2055116917750762

journals.sagepub.com/home/jfmsopenreports

This paper was handled and processed by the European Editorial Office (ISFM) for publication in *JFMS Open Reports*

Toshiyuki Tanaka^{1,2}, Hideo Akiyoshi², Hitoshi Shimazaki^{1,3}, SAGE
Ryo Kawakami⁴, Keiichiro Mie², Yuki Yamada² and Fumihito Ohashi²

Abstract

Case summary This report involves a 10-year-old male mixed-breed cat with a B-cell central nervous system (CNS) lymphoma. The cat presented with ataxia progressing to left hemiparesis. While haematological findings were normal, serum biochemistry showed a high creatine phosphokinase concentration. MRI revealed a homogeneously enhancing well-demarcated extra-axial lesion involving the region of the left lateral aperture with oedema in left flocculus and left medulla oblongata. On diffusion-weighted imaging, the lesion margins showed marked hyperintensity relative to the right cerebellar hemisphere. On an apparent diffusion coefficient map, the lesion appeared hypointense, with an apparent diffusion coefficient value of $0.57 \pm 0.01 \times 10^{-3} \text{ mm}^2/\text{s}$. Cerebrospinal fluid (CSF) analysis and cytology, and genetic analysis of CSF lymphoblasts confirmed a diagnosis of B-cell lymphoma. The owner opted for palliative treatment with prednisolone (1 mg/kg q12h); however, the cat died of dyspnoea 10 days after presentation.

Relevance and novel information CNS lymphomas, which are the second most common intracranial tumours in cats, are highly infiltrative lesions and radical surgical excision is not recommended. Therefore, accurate diagnosis is crucial. However, contrast-enhanced MRI cannot always differentiate these lesions from other conditions, including other CNS tumours and strokes. To the best of our knowledge, this is the first report to document the diffusion-weighted imaging features and apparent diffusion coefficient value for a feline CNS lymphoma. These findings are expected to improve the diagnostic accuracy of these lesions in cats.

Accepted: 27 September 2017

Case description

A 10-year-old male mixed-breed cat was referred to the Kinki Animal Medical Training Institute (KAMTI) for the evaluation of left hemiparesis. Five days earlier, the owner had noticed ataxia progressing to hemiparesis of 2 days' duration. Haematology and serum biochemistry were performed by the referring veterinarian (Next Animal Hospital) and revealed a high creatine phosphokinase concentration (1135 μI ; reference interval 87–309 μI). The cat was negative for feline leukaemia virus but positive for feline immunodeficiency virus (SNAP FeLV/FIV Combo; IDEXX Laboratories). Auscultation of the chest and cardiac ultrasound were normal. Neurological examination at the KAMTI revealed left hemiparesis. The left thoracic and pelvic limb showed no

¹Kinki Animal Medical Training Institute, Osaka, Japan

²Department of Advanced Clinical Medicine, Graduate School of Life and Environmental Sciences, Osaka Prefecture University, Osaka, Japan

³Veterinary Teaching Hospital, Graduate School of Life and Environmental Sciences, Osaka Prefecture University, Osaka, Japan

⁴Next Animal Hospital, Hyogo, Japan

Corresponding author:

Hideo Akiyoshi DVM, PhD, Laboratory of Veterinary Surgery, Department of Graduate School of Life and Environmental Sciences, Osaka Prefecture University, 1-58 Rinku-oraikita, Izumisano-shi, Osaka 598-8531, Japan
Email: akiyoshi@vet.osakafu-u.ac.jp



Creative Commons Non Commercial CC BY-NC: This article is distributed under the terms of the Creative Commons

Attribution-NonCommercial 4.0 License (<http://www.creativecommons.org/licenses/by-nc/4.0/>) which permits non-commercial use, reproduction and distribution of the work without further permission provided the original work is attributed as specified on the SAGE and Open Access pages (<https://us.sagepub.com/en-us/nam/open-access-at-sage>).

response to paw positioning. Withdrawal reflexes and superficial pain nociception were normal. The right thoracic and pelvic limb showed no abnormalities. The cat was non-ambulatory. Mental status and cranial nerve function were normal. Based on neurological examination, a neuroanatomical localisation was suspected in the left medulla oblongata.

Brain MRI was performed on the same day as presentation, using a 1.5 T system (Brivo MR355; GE Healthcare) under general anaesthesia and in a dorsal position. The scanning protocol included transverse fast-spin echo T2-weighted imaging (T2WI), transverse spin echo (SE) T1-weighted imaging (T1WI), fluid-attenuated inversion recovery (FLAIR) imaging and transverse diffusion-weighted imaging (DWI). Transverse DWI included single-shot SE-type echo-planar imaging. T2WI was performed using the following parameters: repetition time (TR)/echo time (TE), 4600/120 ms; thickness, 3.5 mm; spacing, 0.7 mm; number of excitations (NEX), 3; field of view (FOV), 140 mm; matrix, 480 × 480. T1WI was performed using the following parameters: TR/TE, 350/13 ms; thickness, 3.5 mm; spacing, 0.7 mm; NEX, 4; FOV, 140 mm; matrix, 320 × 320; flip angle, 90°. FLAIR imaging was performed using the following parameters: TR/TE, 800/131 ms; inversion time, 2000; thickness, 3.5 mm; spacing, 0.7 mm; NEX, 2; FOV, 140 mm; matrix, 256 × 224. DWI was performed using the following parameters: TR/TE, 3700/88 ms; thickness, 3.5 mm; spacing, 0.7 mm; b-value, 1000 s/mm²; NEX, 4; FOV, 140 mm; matrix, 64 × 64. Diffusion-weighted gradients were applied in three directions (x, y and z). Transverse SE post-contrast T1WI was performed after the administration of gadolinium-diethylenetriamine penta-acetic acid (Magnevist; Bayer) at a dose of 0.2 ml/kg. The apparent diffusion coefficient (ADC) distribution was demonstrated on an ADC colour map created with Functool ver 7.4.03 (GE Healthcare). The ADC value was calculated for multiple regions of interest, excluding cystic and necrosed areas, and values were obtained repeatedly for consistency and reliability of the measurements. ADC values were measured three times and the mean value was calculated.

MRI revealed a well-demarcated extra-axial lesion involving the region of the left lateral aperture (Figure 1d,g,h). The lesion appeared as isointense-to-normal grey matter on T2WI and FLAIR imaging, hypointense on T1WI and homogeneously enhanced on T1WI with contrast (Figure 1a–d). By the lesion, left flocculus and left medulla oblongata revealed mass effect. The left flocculus and left medulla oblongata appeared hyperintense on T2WI and FLAIR imaging, hypointense on T1WI and with no enhancement on T1WI with contrast (Figure 1a–d). The imaging findings were consistent with oedema in left flocculus and left medulla oblongata. On DWI, the lesion margin exhibited marked hyperintensity

relative to the right cerebellar hemisphere (Figure 1e). On the ADC map, the lesion appeared hypointense relative to the right cerebellar hemisphere (Figure 1f). The ADC values for the lesion and the right cerebellar hemisphere were $0.57 \pm 0.01 \times 10^{-3}$ and $1.08 \pm 0.06 \times 10^{-3}$ mm²/s, respectively.

Cerebrospinal fluid (CSF) was collected from the cerebellomedullary cistern. CSF analysis was conducted at a research laboratory (Japan Clinical Laboratories), and the findings revealed an increase in the nucleated cell count to 46/μl (reference interval 0–5/μl). CSF cytology showed the presence of lymphoblasts (Figure 2a), which exhibited a high nuclear:cytoplasmic ratio, basophilic cytoplasm, an irregular nuclear membrane, increased nuclear chromatin and indistinct nuclei. Genetic analysis of the lymphoblasts was conducted at another research laboratory (Canine-Lab); PCR for the assessment of clonality revealed monoclonal proliferation of IgH (Figure 2b). On the basis of these findings, a final diagnosis of B-cell lymphoma was made. The owner of the cat opted for palliative treatment with prednisolone (Mita 1 mg/kg q12h; Kyorin Rimedio). However, the cat died because of dyspnoea 10 days after presentation.

Discussion

In humans, most central nervous system (CNS) lymphomas involve the frontal lobe, corpus callosum and basal nuclei.¹ When precontrast MRI is performed, these lesions appear hypointense or isointense on T1WI and hyperintense or isointense on T2WI. However, the findings of contrast-enhanced MRI are variable.² Frequency of CNS lymphomas with no enhancement is <1%.^{2,3} Therefore, contrast-enhanced MRI cannot always differentiate these lesions from other conditions, including other CNS tumours and strokes.² Furthermore, CNS lymphomas are highly infiltrative and radical surgical excision is not recommended.^{1,4} Because surgical excision is a negative prognostic factor, an accurate diagnosis is crucial.¹ DWI reflects the macromolecular motion of intra- and extracellular water.⁵ ADC distribution, which is measured by DWI, permits quantitative evaluation from images according to the microstructure and pathophysiological state of the tissues.⁶ Because CNS lymphomas are highly cellular, water diffusion is often restricted.⁷ Therefore, they appear hyperintense on DWI and exhibit a decreased ADC value.^{5,7} Restricted diffusion with an ADC threshold value of $\leq 1.1 \times 10^{-3}$ mm²/s has been recommended for the differentiation of CNS lymphoma from other focal intracranial lesions, including tumours and tumour-mimicking lesions.^{5,8}

CNS lymphoma is the second most common intracranial tumour in cats,⁹ presenting as a solitary, well-defined and isolated intraparenchymal mass or a focally extensive infiltrate in the brain.¹⁰ Some animal studies have reported the MRI findings for CNS lymphomas,^{10–12}

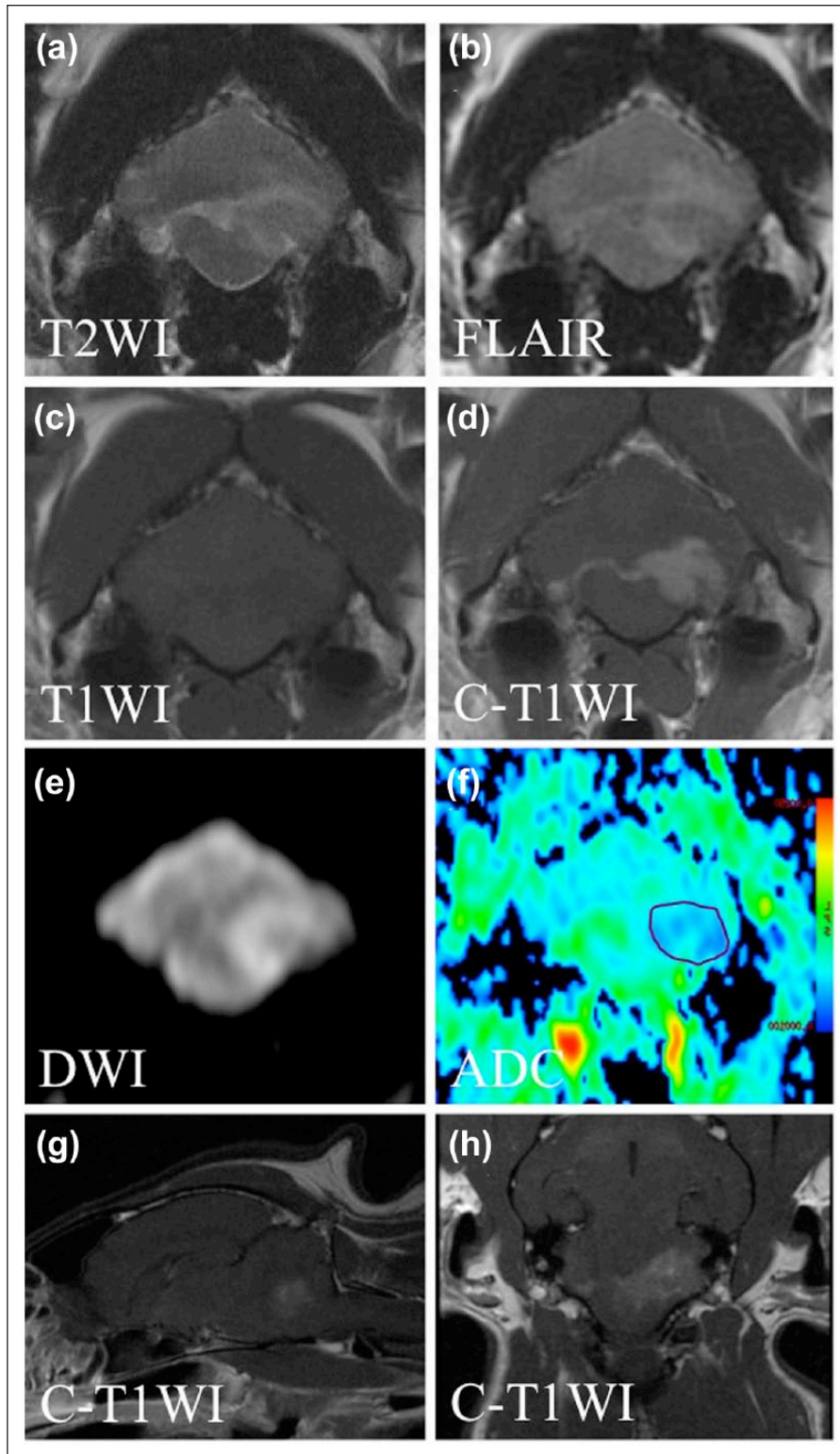


Figure 1 (a–f) Transverse, (g) sagittal and (h) dorsal MRI findings for a B-cell lymphoma involving the region of the left lateral aperture in a 10-year-old male cat. The lesion appears as isointense-to-normal grey matter on (a) T2-weighted imaging (T2WI) and (b) fluid-attenuated inversion recovery imaging, and (c) hypointense on T1-weighted imaging (T1WI). (d,g,h) The lesion is homogeneously enhanced. (e) On diffusion-weighted imaging (DWI), the lesion margin shows remarkable hyperintensity relative to the right cerebellar hemisphere. (f) On the apparent diffusion coefficient (ADC) map, the lesion appears hypointense relative to the right cerebellar hemisphere. The ADC value was calculated for the lesion (circle)

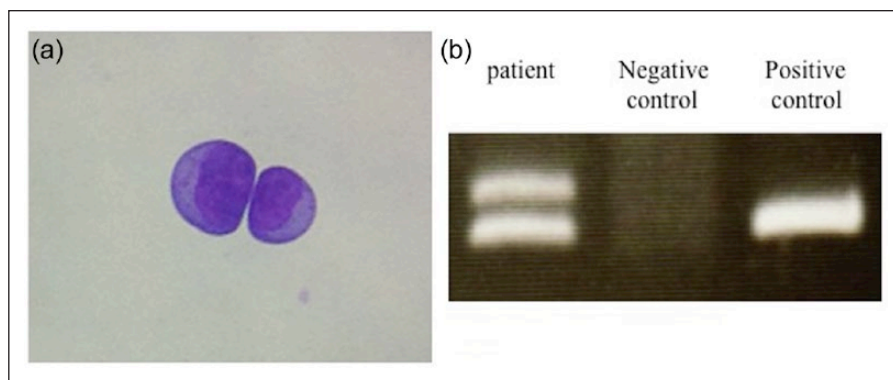


Figure 2 Findings of cerebrospinal fluid (CSF) analysis for a B-cell lymphoma involving the left lobe of the cerebellum in a 10-year-old male cat. (a) CSF cytology shows lymphoblasts with a high nuclear:cytoplasmic ratio, basophilic cytoplasm, an irregular nuclear membrane, increased nuclear chromatin and unclear nuclei (Giemsa staining, $\times 400$). B-cell lymphoma was diagnosed on the basis of genetic analysis of the lymphoblasts. (b) Electrophoresis of PCR products for CSF lymphoblasts revealed monoclonal proliferation of IgH

which are considered non-specific and not diagnostic.^{11,12} Differential diagnoses include non-infectious inflammatory conditions, infectious diseases and other CNS tumours.^{12–14} However, no study has reported the DWI characteristics and ADC value for feline CNS lymphoma. In the present case, the lymphoma appeared hyperintense on DWI, with a decreased ADC value on ADC mapping. These findings may be characteristic findings of CNS lymphomas in cats. Future studies should evaluate a larger number of feline CNS lymphomas.

Definitive diagnosis of intracranial lesions is based on histopathological examination by brain biopsy or CSF examination.^{12,15} Brain biopsy with stereotactic-guided procedures have many advantages.^{15,16} Diagnostic yield is generally $>90\%$ for neoplastic lesions.¹⁵ However, specific equipment is needed to perform brain biopsy. Morbidity and mortality associated with brain biopsy is dependent on the equipment and experience of the operator.¹⁵ Although there are no animal data, sensitivity of CSF examination in human CNS lymphoma is low; lymphoblasts are identified in only about 30%.^{12,17} DWI/ADC by MRI of CNS lymphomas in cats may be a non-invasive diagnostic modality. DWI/ADC needs a high tesla MRI, and this may be a limiting factor for some practitioners.

Conclusions

To the best of our knowledge, this is the first report to document the DWI characteristics and ADC value for a feline CNS lymphoma. Future studies should evaluate a larger number of feline CNS lymphomas with regard to the DWI characteristics, ADC values, and relationship between the ADC value and prognosis.

Conflict of interest The authors declared no potential conflicts of interest with respect to the research, authorship, and/or publication of this article.

Funding The authors received no financial support for the research, authorship, and/or publication of this article.

References

- Zhang D, Hu LB, Henning TD, et al. **MRI findings of primary CNS lymphoma in 26 immunocompetent patients.** *Korean J Radiol* 2010; 11: 269–277.
- Chen H and Dong H. **A rare case of nonenhancing primary central nervous system lymphoma mimic multiple sclerosis.** *Neurosciences* 2015; 20: 380–384.
- Tarae S and Ogata A. **Nonenhancing primary central nervous system lymphoma.** *Neuroradiology* 1996; 38: 34–37.
- Onda K, Wakabayashi K, Tanaka R, et al. **Intracranial malignant lymphomas: clinicopathological study of 26 autopsy cases.** *Brain Tumor Pathol* 1999; 16: 29–35.
- da Rocha AJ, Sobreira Guedes BV, da Silveira da Rocha TM, et al. **Modern techniques of magnetic resonance in the evaluation of primary central nervous system lymphoma: contributions to the diagnosis and differential diagnosis.** *Rev Bras Hematol Hemoter* 2016; 38: 44–54.
- Kuang F, Ren J, Zhong Q, et al. **The value of apparent diffusion coefficient in the assessment of cervical cancer.** *Eur Radiol* 2013; 23: 1050–1058.
- Haldorsen IS, Espeland A and Larsson EM. **Central nervous system lymphoma: characteristic findings on traditional and advanced imaging.** *AJNR Am J Neuroradiol* 2011; 32: 984–992.
- Al-Okaili RN, Krejza J, Woo JH, et al. **Intraaxial brain masses: MR imaging-based diagnostic strategy – initial experience.** *Radiology* 2007; 243: 539–550.
- Troxel MT, Vite CH, Van Winkle TJ, et al. **Feline intracranial neoplasia: retrospective review of 160 cases (1985–2001).** *J Vet Intern Med* 2003; 17: 850–859.
- Guil-Luna S, Carrasco L, Gómez-Laguna J, et al. **Primary central nervous system T-cell lymphoma mimicking meningoencephalomyelitis in a cat.** *Can Vet J* 2013; 54: 602–605.
- Nakamoto Y, Ozawa T, Uchida K, et al. **Primary intra-axial B-cell lymphoma in a cat.** *J Vet Med Sci* 2009; 71: 207–210.

- 12 Palus V, Volk HA, Lamb CR, et al. **MRI features of CNS lymphoma in dogs and cats.** *Vet Radiol Ultrasound* 2012; 53: 44–49.
- 13 Lamb CR, Croson PJ, Cappello R, et al. **Magnetic resonance imaging findings in 25 dogs with inflammatory cerebrospinal fluid.** *Vet Radiol Ultrasound* 2005; 46: 17–22.
- 14 Young BD, Fosgate GT, Holmes SP, et al. **Evaluation of standard magnetic resonance characteristics used to differentiate neoplastic, inflammatory, and vascular brain lesions in dogs.** *Vet Radiol Ultrasound* 2014; 55: 399–406.
- 15 Dickinson PJ. **Advances in diagnostic and treatment modalities for intracranial tumors.** *J Vet Intern Med* 2014; 28: 1165–1185.
- 16 Rossmeis JH, Andriani RT, Cecere TE, et al. **Frame-based stereotactic biopsy of canine brain masses: technique and clinical results in 26 cases.** *Front Vet Sci* 2015; 20: 1–13.
- 17 Fine HA and Mayer RJ. **Primary central nervous system lymphoma.** *Ann Intern Med* 1993; 119: 1093–1104.